

Scattering error corrections for in situ absorption and attenuation measurements

David McKee,^{1,*} Jacek Piskozub² and Ian Brown¹

¹Department of Physics, University of Strathclyde, 107 Rottenrow, Glasgow, G4 0NG, Scotland

²Institute of Oceanology, PAS, ul. Powstancow Warszawy 55, 81-712 Sopot, Poland

*Corresponding author: david.mckee@strath.ac.uk

Abstract: Monte Carlo simulations are used to establish a weighting function that describes the collection of angular scattering for the WETLabs AC-9 reflecting tube absorption meter. The equivalent weighting function for the AC-9 attenuation sensor is found to be well approximated by a binary step function with photons scattered between zero and the collection half-width angle contributing to the scattering error and photons scattered at larger angles making zero contribution. A new scattering error correction procedure is developed that accounts for scattering collection artifacts in both absorption and attenuation measurements. The new correction method does not assume zero absorption in the near infrared (NIR), does not assume a wavelength independent scattering phase function, but does require simultaneous measurements of spectrally matched particulate backscattering. The new method is based on an iterative approach that assumes that the scattering phase function can be adequately modeled from estimates of particulate backscattering ratio and Fournier-Forand phase functions. It is applied to sets of in situ data representative of clear ocean water, moderately turbid coastal water and highly turbid coastal water. Initial results suggest significantly higher levels of attenuation and absorption than those obtained using previously published scattering error correction procedures. Scattering signals from each correction procedure have similar magnitudes but significant differences in spectral distribution are observed.

©2008 Optical Society of America

OCIS codes: (010.4450) Oceanic Optics; (010.1030) Absorption; (010.4458) Oceanic Scattering.

References and links

1. C. D. Mobley, *Light and Water: Radiative Transfer in Natural Waters* (Academic Press, San Diego, Calif., 1994).
2. M. Fujii, E. Boss, and F. Chai, "The value of adding optics to ecosystem models: a case study," *Biogeosciences* **4**, 817-835 (2007). <http://www.biogeosciences.net/4/817/2007/bg-4-817-2007.pdf>
3. S. Maritorena, D. A. Siegel, and A. R. Peterson, "Optimization of a semianalytical ocean color model for global-scale applications," *Appl. Opt.* **41**, 2705-2714 (2002). <http://www.opticsinfobase.org/abstract.cfm?URI=ao-41-15-2705>
4. C. D. Mobley, L. K. Sundman, C. O. Davis, J. H. Bowles, T. V. Downes, R. A. Leathers, M. J. Montes, W. P. Bissett, D. D. R. Kohler, R. P. Reid, E. M. Louchard, and A. Gleason, "Interpretation of hyperspectral remote-sensing imagery by spectrum matching and look-up tables," *Appl. Opt.* **44**, 3576-3592 (2005). <http://www.opticsinfobase.org/abstract.cfm?URI=ao-44-17-3576>
5. D. Stramski and J. Piskozub, "Estimation of Scattering Error in Spectrophotometric Measurements of Light Absorption by Aquatic Particles from Three-Dimensional Radiative Transfer Simulations," *Appl. Opt.* **42**, 3634-3646 (2003). <http://www.opticsinfobase.org/abstract.cfm?URI=ao-42-18-3634>
6. J. Piskozub, D. Stramski, E. Terrill, and W. K. Melville, "Influence of Forward and Multiple Light Scatter on the Measurement of Beam Attenuation in Highly Scattering Marine Environments," *Appl. Opt.* **43**, 4723-4731 (2004). <http://www.opticsinfobase.org/abstract.cfm?URI=ao-43-24-4723>
7. D. Stramski, "Artifacts in measuring absorption spectra of phytoplankton collected on a filter," *Limnol. Oceanogr.* **35**, 1804-1809 (1990). http://aslo.org/lo/toc/vol_35/issue_8/1804.pdf

8. C.S. Roesler, "Theoretical and experimental approaches to improve the accuracy of particulate absorption coefficients derived from the quantitative filter technique," *Limnol. Oceanogr.* **43**, 1649-1660 (1998).
http://www.aslo.org/lo/toc/vol_43/issue_7/1649.pdf
9. J. T. O. Kirk, "Monte Carlo modeling of the performance of a reflective tube absorption meter," *Appl. Opt.* **31**, 6463-6468 (1992).
<http://www.opticsinfobase.org/abstract.cfm?URI=ao-31-30-6463>
10. J. H. M. Hakvoort and R. Wouts, "Monte Carlo modelling of the light field in reflective tube type absorption meter," *Proc. SPIE* **2258**, 529-538 (1994).
11. J. Piskozub, P.J. Flatau, and J.V.R. Zaneveld, "Monte Carlo Study of the Scattering Error of a Quartz Reflective Absorption Tube," *J. Atmos. Oceanic Technol.* **18**, 438-445 (2001).
12. J. R. V. Zaneveld, J. C. Kitchen and C. M. Moore, "The scattering error correction of reflecting-tube absorption meters," *Proc. SPIE* **2258**, 44-55 (1994).
13. D. McKee, A. Cunningham, and S. Craig, "Semi-empirical correction algorithm for AC-9 measurements in a coccolithophore bloom," *Appl. Opt.* **42**, 4369-4374 (2003).
<http://www.opticsinfobase.org/abstract.cfm?URI=ao-42-21-4369>
14. D. McKee and A. Cunningham, "Evidence for wavelength dependence of the scattering phase function and its implication for modeling radiance transfer in shelf seas," *Appl. Opt.* **44**, 126-135 (2005).
<http://www.opticsinfobase.org/abstract.cfm?URI=ao-44-1-126>
15. D. Doxaran, M. Babin, and E. Leymarie, "Near-infrared light scattering by particles in coastal waters," *Opt. Express* **15**, 12834-12849 (2007).
16. P. J. Flatau, J. Piskozub, and J. R. Zaneveld, "Asymptotic light field in the presence of a bubble-layer," *Opt. Express* **5**, 120-123 (1999).
17. Z. Otremba and J. Piskozub, "Modelling of the optical contrast of an oil film on a sea surface," *Opt. Express* **9**, 411-416 (2001).
18. J. M. Sullivan, M. S. Twardowski, J. R. V. Zaneveld, C. M. Moore, A. H. Barnard, P. L. Donaghay, and B. Rhoades, "Hyperspectral temperature and salt dependencies of absorption by water and heavy water in the 400-750 nm spectral range," *Appl. Opt.* **45**, 5294-5309 (2006).
<http://www.opticsinfobase.org/abstract.cfm?URI=ao-45-21-5294>
19. R. M. Pope and E. S. Fry, "Absorption spectrum (380-700 nm) of pure water. II. Integrating cavity measurements," *Appl. Opt.* **36**, 8710-8723 (1997).
<http://www.opticsinfobase.org/abstract.cfm?URI=ao-36-33-8710>
20. R. C. Smith and K. S. Baker, "Optical properties of the clearest natural waters (200-800 nm)," *Appl. Opt.* **20**, 177-184 (1981).
<http://www.opticsinfobase.org/abstract.cfm?URI=ao-20-2-177>
21. C. D. Mobley, L. K. Sundman, and E. Boss, "Phase Function Effects on Oceanic Light Fields," *Appl. Opt.* **41**, 1035-1050 (2002).
<http://www.opticsinfobase.org/abstract.cfm?URI=ao-41-6-1035>
22. J. L. Forand and G. R. Fournier, "Particle distributions and index of refraction estimation for Canadian waters," *Proc. SPIE* **3761**, 34-44 (1999).
23. W. Freda and J. Piskozub, "Improved method of Fournier-Forand marine phase function parameterization," *Opt. Express* **15**, 12763-12768 (2007).
24. M. Jonasz and G. Fournier, "Approximation of the size distribution of marine particles by a sum of log-normal functions," *Limnol. Oceanogr.* **41**, 744-754 (1996).
25. D. Risović, "Effect of suspended particulate-size distribution on the backscattering ratio in the remote sensing of seawater," *Appl. Opt.* **41**, 7092-7101 (2002).
<http://www.opticsinfobase.org/ao/abstract.cfm?URI=ao-41-33-7092>
26. M. Chami, D. McKee, E. Leymarie, and G. Khomenko, "Influence of the angular shape of the volume-scattering function and multiple scattering on remote sensing reflectance," *Appl. Opt.* **45**, 9210-9220 (2006).
<http://www.opticsinfobase.org/ao/abstract.cfm?URI=ao-45-36-9210>

1. Introduction

Inherent optical properties (IOPs) such as absorption (a), scattering (b) and attenuation (c) are essential inputs for radiative transfer (RT) models for underwater light fields that are of increasing importance for ecosystem modelling applications [1,2]. IOPs and RT simulations are also used for interpreting remote sensing signals from satellite-borne ocean colour sensors [3,4]. IOPs are, however, generally difficult to measure precisely as it is practically impossible to design sensors that fully collect all scattered photons for absorption measurements [5], or fully exclude all scattered photons for attenuation measurements [6]. In this paper we use Monte Carlo simulations to examine the collection of scattered photons in a reflecting tube absorption meter modeled on a commercially available and widely used instrument, the WETLabs Inc. AC-9. The AC-9 (and latterly AC-S) has become an important oceanographic

tool for generating in situ a and c data (and $b = c - a$) with unprecedented temporal / spatial frequency. Using samples pumped directly through enclosed flow tubes, the AC-9 avoids sample handling and pathlength amplification artifacts associated with absorption measurements made on filtered samples [7,8]. Absorption is measured with a reflecting tube and a large area diffusing collector that is intended to collect as many scattered photons as possible. Attenuation is measured with a traditional transmissometer design that excludes photons scattered outside a narrow range of forward scattering angles. Several studies have examined various aspects of these designs including optimization of flow tube diameter and reflecting materials for the absorption tube, effects of multiple scattering and potential errors in attenuation measurements through incomplete exclusion of forward scattering [5,6,9-11]. Zaneveld et al proposed a scattering correction procedure for the reflecting tube absorption meter that could be implemented without additional optical information external to the AC-9 [12]. In order to achieve this self-contained correction procedure, Zaneveld et al had to assume that the scattering phase function was wavelength independent and that absorption in the NIR was negligible. Recent studies have questioned the general validity of these assumptions and noted potential artifacts in AC-9 data corrected using this procedure [13-15]. The purpose of this study is to use Monte Carlo simulations of the AC-9 to establish a detailed understanding of the angular scattering collection characteristics of both channels of the instrument and to use this to inform a new procedure for correcting measurements of a and c for scattering collection errors. In this process we will take advantage of the introduction of new backscattering meters (e.g. the WETLabs BB-9) that were unavailable when the Zaneveld et al procedure was developed, and include spectrally matched particulate backscattering (b_{bp}) as a variable that can be used in the new correction procedure.

2. Theory

The WETLabs AC-9 measures both absorption and attenuation by materials other than water. Both measurements are subject to scattering errors as a result of practical limitations of sensor geometry. The absorption sensor fails to collect all scattered light and the attenuation sensors fails to exclude all scattered photons so that true non-water absorption (a_n) and attenuation (c_n) signals are given by

$$a_n(\lambda) = a_m(\lambda) - \varepsilon_a(\lambda) \quad (1)$$

$$c_n(\lambda) = c_m(\lambda) + \varepsilon_c(\lambda) \quad (2)$$

where a_m and c_m are measured absorption and attenuation, and ε_a and ε_c are scattering errors for absorption and attenuation. These scattering errors can be written as

$$\varepsilon_a(\lambda) = f_a(\lambda)b_p(\lambda) \quad (3)$$

$$\varepsilon_c(\lambda) = f_c(\lambda)b_p(\lambda) \quad (4)$$

where b_p is the true scattering coefficient, f_a is the fraction of scattered light not collected by the absorption sensor and f_c is the fraction of scattered light that is collected by the attenuation sensor. f_a is given by

$$f_a(\lambda) = 2\pi \int_0^\pi W_a(\psi) \tilde{\beta}_p(\lambda, \psi) \sin\psi \, d\psi \quad (5)$$

where $\tilde{\beta}_p$ is the wavelength dependent scattering phase function and W_a is a wavelength independent weighting distribution function that describes the angular scattering collection efficiency of the absorption sensor [5]. Piskozub et al have shown that the equivalent weighting function for attenuation sensors is reasonably approximated by assuming that all photons scattered between zero and the collection angle of the transmissometer (ψ_c) contribute

equally to the attenuation scattering error and that photons scattered outside this range make zero contribution to the error [6 – see Table 1 in that paper]. This was confirmed with Monte Carlo simulations (not shown) for the AC-9 attenuation sensor configuration. f_c is therefore given by the cumulative phase function from zero to ψ_c

$$f_c(\lambda) = 2\pi \int_0^{\psi_c} \tilde{\beta}_p(\lambda, \psi) \sin \psi \, d\psi \quad (6)$$

As the true particulate scattering is given by $b_p(\lambda) = c_n(\lambda) - a_n(\lambda)$, Eq. (1)-(4) can be used to demonstrate that

$$b_p(\lambda) = \frac{b_m(\lambda)}{1 - f_a(\lambda) - f_c(\lambda)} = E_b(\lambda)b_m(\lambda) \quad (7)$$

It is then simple to show that

$$a_n(\lambda) = a_m(\lambda) - \frac{f_a(\lambda)b_m(\lambda)}{[1 - f_c(\lambda) - f_a(\lambda)]} = a_m(\lambda) - E_a(\lambda)b_m(\lambda) \quad (8)$$

$$c_n(\lambda) = c_m(\lambda) + \frac{f_c(\lambda)b_m(\lambda)}{[1 - f_c(\lambda) - f_a(\lambda)]} = c_m(\lambda) + E_c(\lambda)b_m(\lambda) \quad (9)$$

where $E_a(\lambda)$, $E_b(\lambda)$ and $E_c(\lambda)$ are error weighting functions that permit correction of each signal with the measured scattering, $b_m(\lambda)$. These functions are given by

$$E_a(\lambda) = \frac{f_a(\lambda)}{1 - f_c(\lambda) - f_a(\lambda)} \quad (10)$$

$$E_b(\lambda) = \frac{1}{1 - f_c(\lambda) - f_a(\lambda)} \quad (11)$$

$$E_c(\lambda) = \frac{f_c(\lambda)}{1 - f_c(\lambda) - f_a(\lambda)} \quad (12)$$

3. Methods

Monte Carlo simulations were performed with code previously used to study ocean optics phenomena and instrumentation [5, 6, 16, 17]. The AC-9 absorption and attenuation sensors were simulated using accurate instrument dimensions provided by the manufacturer. The pathlength of each sensor (τ) was 0.25m. The transmissometer had a scattering collection half-width angle of 0.9 and the absorption sensor was modeled as a first order cosine detector using a 90° step-function. Simulations were performed for 10^8 photons per run and the following IOPs: $a = 0.006 \text{ m}^{-1}$, $b = 0.25 \text{ m}^{-1}$, and a Henyey-Greenstein phase function with an asymmetry parameter of 0.8. These IOPs were selected to ensure that the optical thickness ($c \cdot \tau$) was less than 0.3 so that multiple scattering could be ignored. The Henyey-Greenstein phase function was chosen as a means of ensuring sufficient numbers of photons would be scattered into each angular bin to reduce the inherent statistical error of the Monte Carlo approach. It was selected as a compromise between other, more realistic phase functions for natural waters and an isotropic phase function that would have been preferable from the point of view of calculation statistics. It has previously been rigorously demonstrated that the W_a function is independent of the IOPs and phase function used in the Monte Carlo simulations [5]. This was confirmed for the AC-9 configuration by performing a number of Monte Carlo

simulations for a small number of alternative values of IOPs and scattering phase functions. The derived W_a function can therefore be used with other combinations of IOPs and phase functions without further modification, with the possible exception of strongly multiple scattering waters.

In situ IOP measurements were made with WETLabs AC-9 (a and c) and BB-9 (b_b) sensors in clear ocean waters of the sub-tropical Atlantic Ocean, moderately turbid waters of the Irish Sea and in highly turbid waters of the Bristol Channel. All data were processed into 1m bin averages. The AC-9 was calibrated with 0.2 μ m filtered Milli-Q ultrapure water. AC-9 measurements were corrected for salinity and temperature using data from a Seabird SBE 19plus CTD and coefficients from Sullivan et al [18]. A series of scattering corrections were performed for later comparison, including: no correction (nobc), the Zaneveld et al correction (zane), a spectrally flat baseline assuming $a_n(715) = 0 \text{ m}^{-1}$ (flat), and the new iterative scattering correction developed here (iter). Backscattering data were corrected for pathlength absorption effects using absorption data from the AC-9 corrected using the Zaneveld method. Absorption and scattering coefficients for pure water were taken from Pope and Fry, and Smith and Baker respectively [19,20]. Spectral matching between AC-9 and BB-9 data was achieved by interpolating BB-9 data to match AC-9 wavelengths where necessary.

4. Results

Monte Carlo simulations of the AC-9 absorption tube were used to determine the weighting distribution function for uncollected scattered photons W_a as a function of scattering angle (Fig. 1). The results indicate that scattered photons are efficiently collected up to scattering angles of $\sim 41^\circ$ (the critical angle for total internal reflection for the submerged flow tube), but very poorly for greater scattering angles. The small improvement in scattering collection from 140° to 180° is due to backscattered photons reflecting off the input window and reaching the detector at the forward end of the tube. The step between $\sim 15^\circ$ and 41° is harder to interpret, but is potentially due to details in the optical geometry of the system, including detector size relative to tube diameter, and length of the gap between the end of the flow tube and the detector window (1 cm). It should be noted that this weighting function has been generated for single scattering environments and may not hold for more turbid water where multiple scattering could affect collection efficiency.

The absorption weighting distribution function, W_a , was used in Eq. (5), together with Fournier-Forand phase functions calculated using the parameterisation of Mobley et al [21], to calculate values of fraction of scattered light not collected by the absorption sensor, f_a , as a function of particulate backscattering ratio (Fig. 2). Also shown is the fraction of scattered light collected by the attenuation sensor, f_c , calculated from cumulative Fournier-Forand phase functions between 0 and 0.9° for the range of particulate backscattering ratios encountered in natural waters. Cumulative Fournier-Forand phase functions were calculated using the expressions provided by Forand and Fournier [22], analogous to Eq. (6). Best-fit lines in Fig. 2 facilitate estimation of f_a (4th order polynomial) and f_c (3-parameter hyperbolic decay) as functions of b_{bp}/b_p .

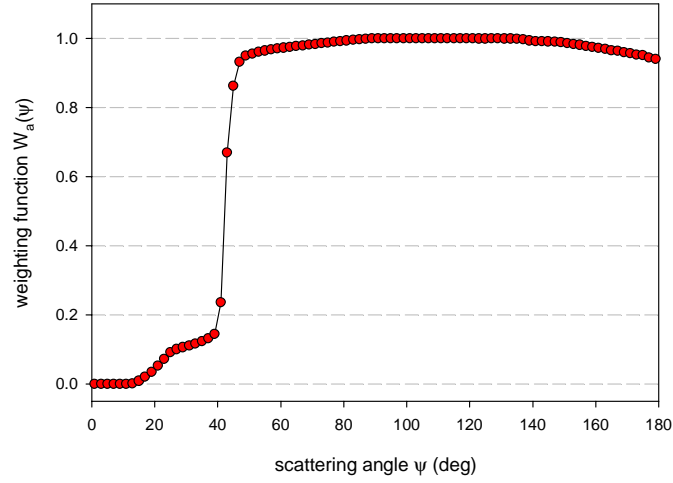


Fig. 1. Weighting distribution function for AC-9 reflective tube absorption meter. Zero indicates all photons collected by sensor, unity means no photons collected from this scattering angle.

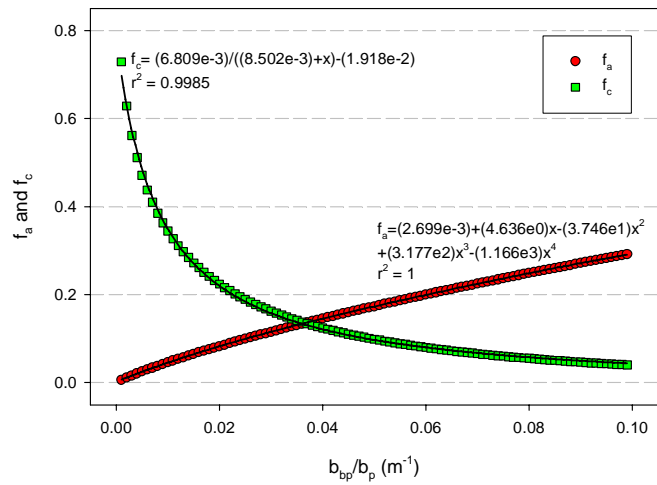


Fig. 2. Fraction of scattered light uncollected by the AC-9 absorption sensor, f_a , and fraction of scattered light collected by the AC-9 attenuation sensor, f_c , for Fournier-Forand phase functions calculated with the method proposed by Mobley et al [21].

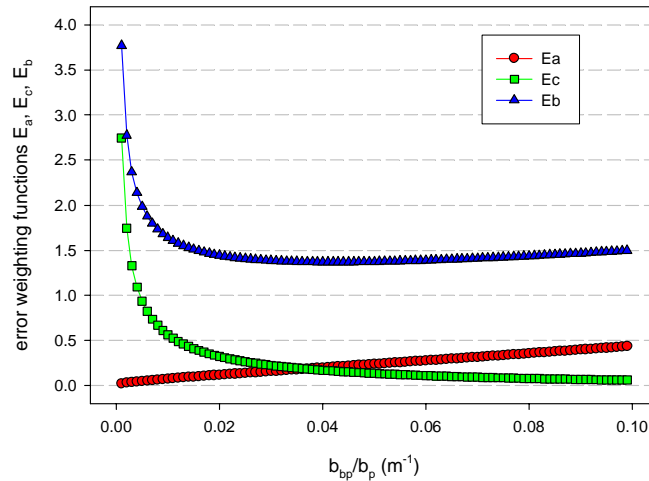


Fig. 3. Error weighting functions for absorption, attenuation and scattering signals calculated from f_a and f_c values as functions of particulate backscattering ratio.

Figure 3 shows error weighting functions for calculating correct values of non-water absorption, attenuation and scattering using Eqs. (10)-(12). E_a increases almost linearly as the particulate backscattering ratio increases, while E_c is large for strongly forward scattering waters but drops to lower values when the particulate backscattering ratio increases. E_b is large (>2) for $b_{bp}/b_p < 0.005$, but is relatively stable within the range 1.35 – 2 for $b_{bp}/b_p > 0.005$.

5. Discussion

Monte Carlo simulations of the AC-9 absorption and attenuation tubes enabled estimation of fractional scattering collection of each sensor as functions of the particulate backscattering ratio (Fig. 2). In order to use this information to correct AC-9 signals one has to be able to estimate b_{bp}/b_p . However, since this involves use of particulate scattering, b_p , a potential logical circularity is encountered (for simplicity we shall ignore the use of absorption signals in correcting b_{bp} data for small pathlength attenuation effects, but note that this could be incorporated as an additional step at a future date). This problem can be overcome by adopting an iterative scattering error correction approach whose steps are outlined in Fig. 4. Steps include: initial estimate of b_p using a typical value of $E_b = 1.5$, initial estimation of b_{bp}/b_p leading to estimates of c_n and a_n , and iteration until b_{bp}/b_p reaches a stable value within a set tolerance. The choice of tolerance is arbitrary, but should be sufficiently small to ensure adequate parameterisation of f_a and f_c , and large enough to facilitate closure within a reasonable number of iterations. A threshold of 0.001 was chosen for initial testing.

This iterative scattering correction procedure was applied to in situ AC-9 and BB-9 data from three sites representative of clear ocean, moderately turbid shelf sea and highly turbid coastal waters.

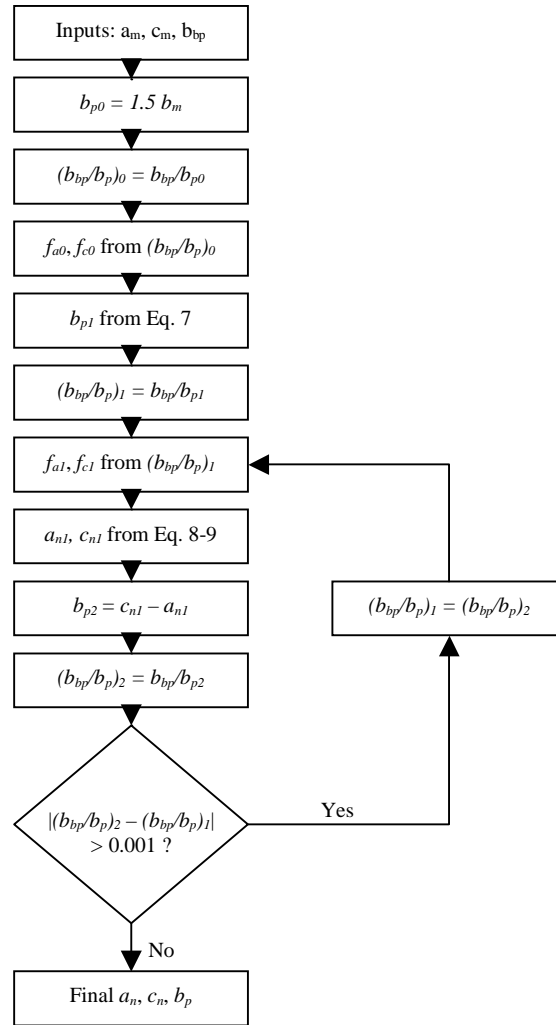


Fig. 4. Flowchart of steps in iterative scattering correction procedure.

5.1 Clear ocean station

Figure 5 shows AC-9 spectra collected from a station in the sub-tropical North Atlantic Ocean near the Canary Islands in January 2008. Data are shown after correction for temperature and salinity effects and 1 m bin averaging. Output from the iterative scattering correction procedure (iter) can be compared with data with: no scattering correction (nobc), the Zaneveld et al scattering correction (zane) and a spectrally flat baseline correction assuming $a_n(715) = 0 \text{ m}^{-1}$ (flat). The most striking feature of the iterative correction data is non-zero absorption at 715 nm. In fact only ~50% of the residual (nobc) absorption signal at 715 nm is attributed to scattering using the iterative scattering correction procedure. This gives $a_n(715)$ values of $\sim 0.005 \text{ m}^{-1}$ when $a_n(440) \approx 0.030 \text{ m}^{-1}$. Attenuation signals are also generally $\sim 0.005 \text{ m}^{-1}$ higher for the iterative data than for the other methods. This results in scattering signals with generally similar magnitudes from each scattering procedure. However, close inspection reveals subtle differences in spectral shape, with the iterative correction scattering data suggesting slightly stronger dips at wavelengths where anomalous dispersion effects occur (e.g. 440 nm).

5.2 Moderately turbid shelf sea station

Figure 6 shows AC-9 data from a moderately turbid station from the Irish Sea. All four correction procedures previously identified have been applied to the data and are shown. Again, only ~50% of the residual absorption (nbc) measured at 715nm is attributed to scattering using the iterative correction method, leaving final estimates of $a_n(715)$ of ~ 0.05 to 0.08 m^{-1} when $a_n(440) = 0.2 \text{ m}^{-1}$. Absorption data at blue wavelengths is generally higher by ~ 0.1 m^{-1} using the iterative correction procedure rather than the Zaneveld et al approach. Iterative attenuation signals are higher by a similar amount than Zaneveld et al values, leaving scattering signals with roughly equivalent magnitudes. As previously, there are interesting differences in the spectral characteristics of the scattering signals, particularly in the blue where absorption signals are strongest. This is an area with strong mineral particle absorption where one might expect to see significant anomalous dispersion at blue wavelengths. The attenuation signals at this station are at the limit of the domain where multiple scattering is not dominant for a 25 cm pathlength instrument.

5.3 Highly turbid coastal station

The final data set (Fig. 7) is from a highly turbid station in the Bristol Channel. The attenuation signals from this station ($c_n \approx 3 \text{ m}^{-1}$) indicate that multiple scattering would significantly influence the propagation of photons along a 25 cm path. Consequently, it is possible that the weighting distribution functions determined previously may not be adequate for this degree of turbidity. However, it is interesting to note that there does not appear to be any catastrophic failure of the iterative method even for such highly turbid waters. The iterative scattering correction procedure gives values of $a_n(715) \approx 0.4 \text{ m}^{-1}$, approximately 60% of the residual measured absorption (nbc) before scattering correction. Iterative absorption and attenuation signals are both greater by similar amounts (~ 0.5 m^{-1} in the blue) than equivalent signals processed using either the flat baseline or Zaneveld et al correction procedures, leaving scattering signals with similar magnitudes. Scattering signals from the iterative scheme again have a noticeably different spectral shape, particularly at blue wavelengths where anomalous dispersion effects could be significant for waters with strong mineral absorption.

5.4 Analysis

Initial results from the iterative scattering correction procedure indicate that absorption at 715 nm may be non-zero, even in reasonably clear ocean waters. This result is consistent with other measurements of absorption from e.g. filter pad spectrophotometry, where decreases in absorption from 715 nm to 750 nm are often observed. In phytoplankton dominated water, the peak at 676 nm associated with chlorophyll *a* is often sufficiently pronounced that absorption at 715 nm is on the slope of the peak rather than the baseline. Likewise, filter pad absorption spectra from stations with high mineral particle loading often show absorption decreasing from 715 nm to 750 nm. The results presented here, however, go further than filter pad absorption measurements which are usually set to zero at 750 nm. The iterative AC-9 correction procedure does not assume zero absorption at any wavelength, and would be well suited for in situ measurements further into the NIR, particularly in turbid coastal waters [15].

Data from each of the case studies indicate substantial differences in the magnitude of retrieved absorption and attenuation depending on the selection of scattering error correction method. The magnitude of such differences vary with the scattering signal, Eqs. (8)-(9), but are potentially significant for applications such as radiative transfer simulations. In clear waters for example, a difference in blue absorption of 0.01 m^{-1} (Fig. 5) actually represents an increase of 50% from the equivalent Zaneveld et al value. In highly turbid water (Fig. 7) the iterative procedure suggests non-water absorption values at 715 nm that are a significant fraction (30-50%) of the absorption by water itself.

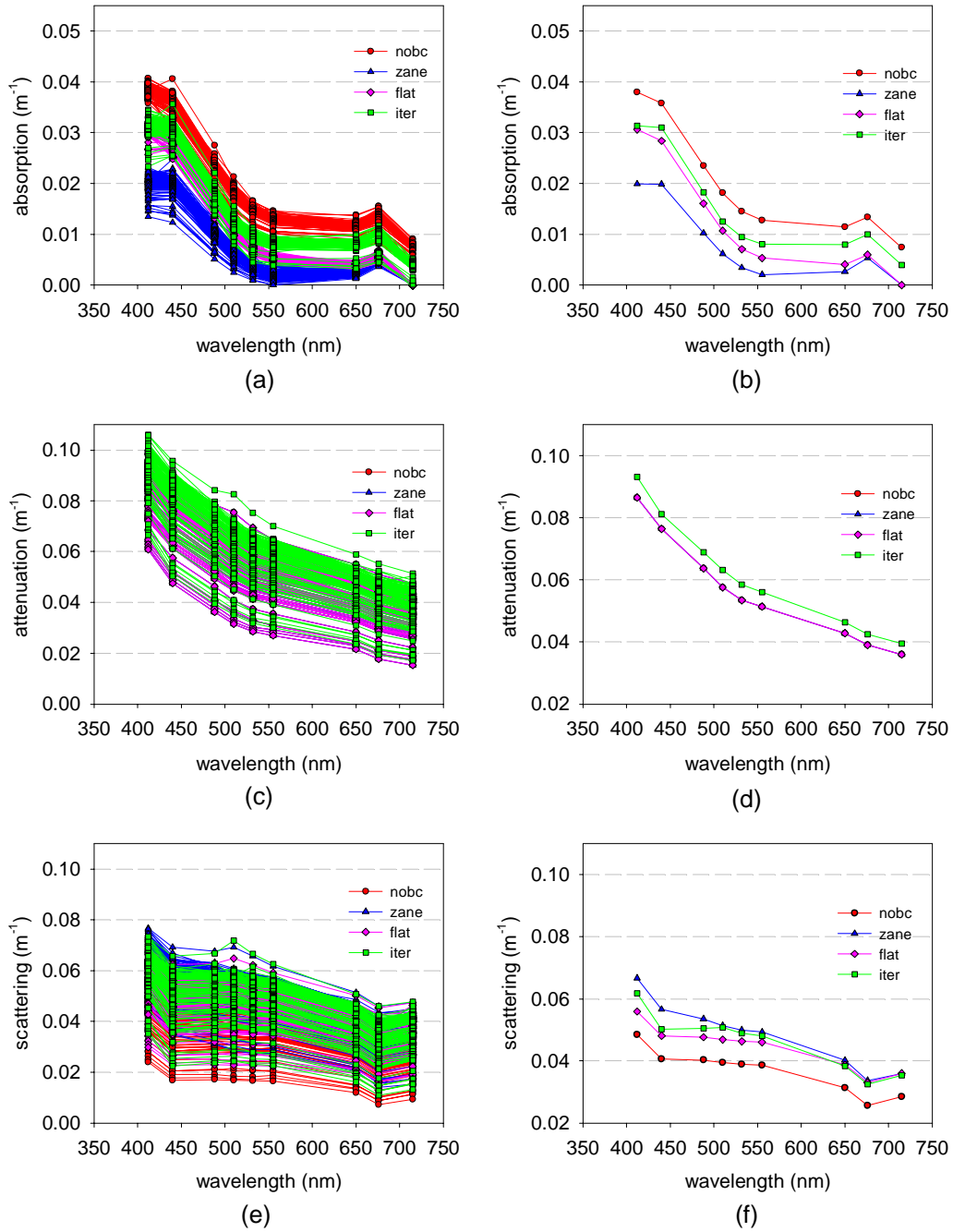


Fig. 5. AC-9 data from a clear ocean station in the sub-tropical North Atlantic Ocean with four different scattering error correction methods applied. (a), (c) and (e) data from 1m bin averages from a single depth profile. (b), (d) and (f) mean spectra from the same depth profile.

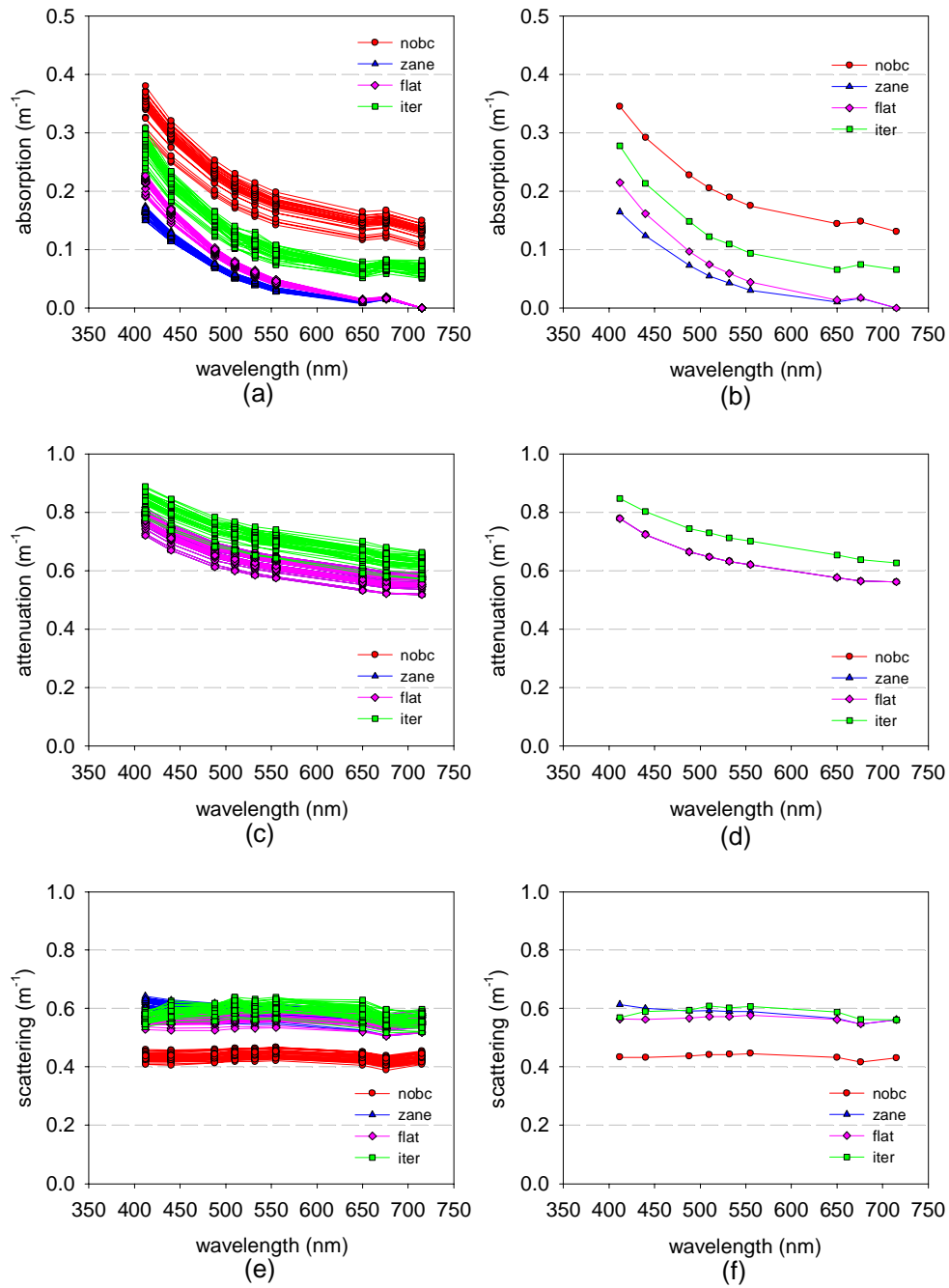


Fig. 6. AC-9 data from a moderately turbid station in the Irish Sea, with four different scattering error correction methods applied. (a), (c) and (e) data from 1m bin averages from a single depth profile. (b), (d) and (f) mean spectra from the same depth profile.

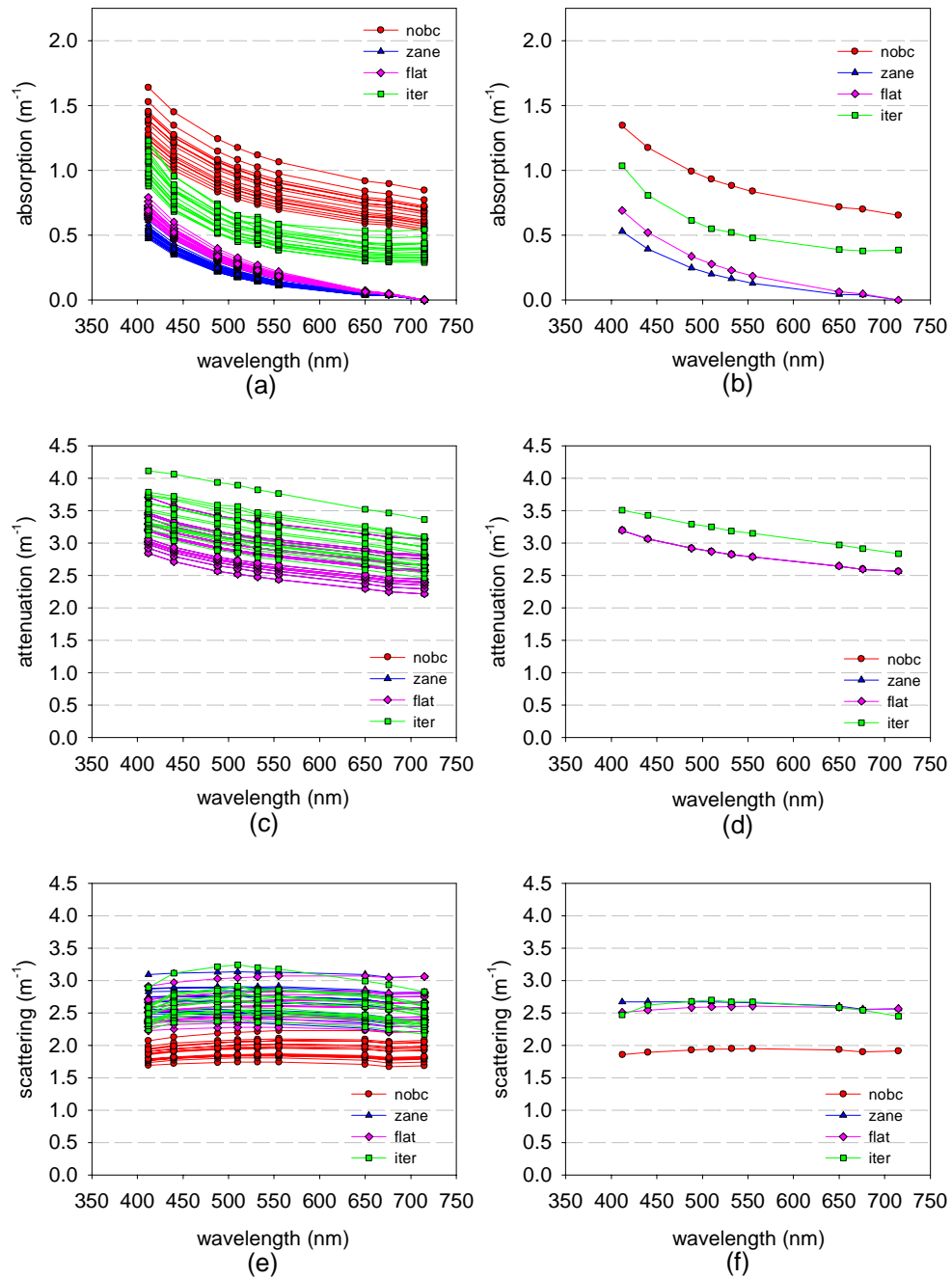


Fig. 7. AC-9 data from a highly turbid station in the Bristol Channel, with four different scattering error correction methods applied. (a), (c) and (e) data from 1m bin averages from a single depth profile. (b), (d) and (f) mean spectra from the same depth profile.

Differences in spectral distributions of IOPs between scattering correction methods are a little harder to interpret. The iterative correction procedure does not assume zero non-water absorption in the NIR, and does not assume wavelength independence for the scattering phase function. Removing each of these constraints has an impact on retrieved spectral distributions. The fact that spectral scattering from the iterative procedure is consistent with known features of the particles in suspension for each case is good circumstantial evidence that the procedure is reasonably well behaved. Further validation is required to establish if the iterative correction procedure provides any substantial improvement in the quantitative quality of IOP spectra. This will be determined through optical closure studies using concurrent radiometry and radiative transfer simulations of the underwater light field [13,14].

6. Conclusions

3D Monte Carlo simulations have been used to provide a new insight into the scattering collection performance of the AC-9 reflecting tube absorption meter. Previous Monte Carlo simulations enabled similar characterisation of the beam transmissometer optics [6]. By establishing a new parameterisation of the scattering collection performance of both sensors, it has been possible to develop an iterative scattering error correction procedure that does not assume zero absorption in the NIR and makes no assumption about wavelength dependence of the scattering phase function. The iterative procedure requires simultaneous measurements of particulate backscattering and uses the Mobley et al parameterisation for Fournier-Forand phase functions [21]. It should be noted, however, that alternative scattering phase functions could be assimilated into the procedure if necessary [23]. For example, Fournier-Forand phase functions are based on an assumption of a power law particle size distribution whose validity has been challenged in a number of studies, e.g. [24, 25]. Sensitivity of the iterative correction procedure to angular structure in the scattering phase function is an area requiring further study [26]. The iterative procedure uses a scattering weighting function that was derived for water where multiple scattering is not significant. This could be a limiting feature of the procedure, but initial results from turbid water with strong multiple scattering suggest that it may be sufficiently robust for high scattering waters.

Application of the iterative scattering correction procedure to in situ data from natural waters with a range of turbidities revealed consistent differences with data derived using other scattering error correction protocols. The iterative procedure produced higher absorption and attenuation signals, and scattering signals with generally similar magnitudes but different spectral distributions. Approximately 50 – 60% of residual absorption signals at 715 nm prior to scattering correction were found to attributable to scattering error, whereas other correction procedures assume that 100% of this signal is due to scattering error.

The iterative scattering error correction procedure is presented for consideration as an alternative to other established correction methods. It is based on sound theoretical considerations and Monte Carlo simulations of the AC-9 instrument using detailed descriptions of the optical configurations provided by the manufacturer. Potential users should be aware of the limitations and assumptions discussed above. The iterative scattering correction procedure may be a step towards higher quality in situ IOP measurements. The results from Monte Carlo simulations of the optical configurations that underpin the iterative correction procedure are certainly a step forward in our understanding of the performance of these optical designs.

Acknowledgments

This work was supported by awards to McKee and Piskozub under the International Exchange Programme funded by the Polish Academy of Sciences and the Royal Society of Edinburgh. McKee is also supported by a NERC Advanced Fellowship. Piskozub is supported by IOPAS statutory research project I.3. The authors would like to thank colleagues from WETLabs Inc. for providing detailed advice on optical configurations for the AC-9 instrument.